

Next-to-leading order QCD corrections to spin-dependent hadron-pair photoproduction

C. Hendlmeier¹, A. Schäfer¹, and M. Stratmann²

¹ Institut für Theoretische Physik, Universität Regensburg, D-93040 Regensburg, Germany

² Radiation Laboratory, RIKEN, 2-1 Hirosawa, Wako, Saitama 351-0198, Japan

Abstract. We compute the next-to-leading order QCD corrections to the “direct” part of the spin-dependent cross section for hadron-pair photoproduction. The calculation is performed using largely analytical methods. We present a brief phenomenological study of our results focussing on the K -factors and scale dependence of the next-to-leading order cross sections. This process is relevant for the extraction of the gluon polarization in present and future spin-dependent lepton-nucleon scattering experiments.

PACS. 13.88.+e – 12.38.Bx – 13.85.Ni

1 Introduction and Motivation

For many years the field of QCD spin physics has been driven by the hugely successful experimental program of polarized deeply-inelastic lepton-nucleon scattering (DIS). One of the most prominent results has been the finding that quarks and anti-quarks summed over all flavors, $\Delta\Sigma$, provide only about a quarter of the nucleon’s spin, contrary to naive expectations from quark models. This implies that sizable contributions to the nucleon spin should come from the polarization of gluons, $\Delta g(Q^2)$, or from orbital angular momenta $L_{q,\bar{q},g}(Q^2)$ of partons. Here, Q denotes the resolution scale at which the nucleon is probed.

Results from fully inclusive DIS experiments are now supplemented by a growing amount of data from polarized proton-proton collisions at BNL-RHIC [1], but also from less inclusive measurements in lepton-nucleon scattering [2, 3, 4, 5]. Determining the gluon spin contribution is the major focus of all these experiments. The strength of RHIC is the possibility to study several different processes over a wide kinematical range which are directly sensitive to gluon polarization [6]: single-inclusive prompt photon, jet, hadron, and heavy flavor production at high transverse momentum p_T or any combination of these final-states in two-particle correlations. The way to access $\Delta g(Q^2)$ in lepton-nucleon scattering is to select final-states which are predominantly produced through the photon-gluon fusion (PGF) process. Due to the relatively small center-of-mass system (c.m.s.) energy \sqrt{S} available in current fixed-target experiments, such studies are limited to charm and single- or di-hadron production at moderate p_T .

To reliably determine of the amount of gluon polarization $\Delta g(Q^2)$ entering the proton helicity sum rule, it is imperative to precisely map its Bjorken- x dependence

first, in order to minimize extrapolation uncertainties in

$$\Delta g(Q^2) \equiv \int_0^1 \Delta g(x, Q^2) dx \quad . \quad (1)$$

The eventual extraction of $\Delta g(x, Q^2)$ will require consideration of *all* existing data through a “global QCD analysis” that makes simultaneous use of results for all probes, from pp and from lN scattering. This is the only way to effectively deconvolute the experimental information, which in its raw form is smeared over the fractional gluon momentum x and is taken at different scales Q .

The basic concept that underlies the theoretical framework for high- p_T processes, and any global analysis thereof, is the factorization theorem. It states that large-momentum transfer reactions may be factorized into long-distance pieces that contain the desired information on the spin structure of the nucleon in terms of universal parton densities $\Delta f(x, Q^2)$, $f = q, \bar{q}, g$, and parts that describe the short-distance, hard interactions of the partons. The latter can be evaluated within perturbative QCD. Here, at least next-to-leading order (NLO) accuracy is required for quantitative analyses to control theoretical uncertainties.

A first such global QCD analysis of $\Delta f(x, Q^2)$ is now well under way [7], including all recent results from the RHIC experiments PHENIX and STAR [1]. However, results on hadron-pair production from polarized lepton-nucleon scattering experiments [3, 4] have to be left out due to the complete lack of NLO computations for this important class of processes. Two-hadron photoproduction is also expected to play an important role in the spin physics program at a future polarized lepton-proton collider, which is currently under discussion [8].

This paper is the first step towards a full NLO description of hadron-pair production in longitudinally polarized lepton-nucleon collisions. Here, we compute the

NLO QCD corrections to the “direct” part of the spin-dependent cross section for two-hadron photoproduction,

$$l(P_l, \lambda_l)N(P_N, \lambda_N) \rightarrow l'(P_{l'})H_1(P_1)H_2(P_2)X, \quad (2)$$

i.e., where the exchanged photon is at low virtuality and interacts as an elementary particle with one of the partons of the nucleon N . The P_i in (2) are the four-momenta of the observed leptons and hadrons, X contains all the additional hadronic activity not observed in experiment, and the λ_i denote the helicities of the interacting lepton l and nucleon N .

Of course, an immediate complication arises here, as the direct part on its own is no longer a well-defined quantity beyond the leading order (LO) approximation. This is due to kinematical configurations with a collinear splitting of the photon into a $q\bar{q}$ pair which need to be factorized into the photon structure functions appearing in the “resolved” part of the cross section. This is well-known [9] and expresses the freedom in the factorization procedure such that only the sum of direct and resolved contributions is independent of theoretical conventions. Nevertheless, we will concentrate in this work on the direct part of the polarized two-hadron production cross section which is technically already rather involved.

This is because we perform the calculation using largely analytical methods. Calculations of this kind were pioneered in the unpolarized case for photon-hadron [10], photon-photon [11], and photon-charm [12] correlations quite some time ago. In the polarized case only a calculation for double-photon production [13] exists so far. To keep the computations tractable, we chose to present the results in terms of the transverse momentum and rapidity of “hadron one” (H_1), $P_{T,1}$ and y_1 , respectively, and a variable [10,11]

$$z_H \equiv -\frac{\mathbf{P}_{T,1} \cdot \mathbf{P}_{T,2}}{P_{T,1}^2} \quad (3)$$

which contains some information about the kinematics of “hadron two”, H_2 , but not including its rapidity y_2 . Numerical evaluations of the triple differential cross section are thus limited in that experimental cuts on the rapidity of the second hadron H_2 cannot be implemented. The introduction of z_H in the analytical calculation is essential to keep certain singular configurations at bay [10,11], for instance, the case when the two hadrons are produced collinearly, as will be discussed in more detail below.

Despite the fact that our calculation is not complete in the sense discussed above, we strongly believe our results to be very important, both theoretically and phenomenologically. On the one hand, our results will serve as a check on more versatile calculations in the future using combined analytical and Monte Carlo techniques which we are pursuing at the moment [14] along similar lines as in the unpolarized case [15]. These studies [14] will include also the spin-dependent resolved photon contributions at NLO accuracy. On the other hand, it was demonstrated in recent a LO study [16] that the direct photon part is responsible for the main features of the experimentally relevant spin asymmetry and its sensitivity to the polarized

gluon density at fixed-target experiments like COMPASS and HERMES. The resolved photon part is non-negligible though, but merely leads to a roughly constant shift of the spin asymmetries. We also believe that our numerical studies of the relevance of the NLO corrections and theoretical uncertainties due to variations of the factorization and renormalization scales already give a good indication of what to expect from a full NLO calculation in the future.

The paper is organized as follows: in Sec. 2 we present the details of the calculation of the NLO QCD corrections to the direct part of spin-dependent two-hadron photoproduction. Section 3 is devoted to a brief numerical evaluation of our results, focussing on the relevance of the NLO corrections and the residual scale uncertainties at fixed-target kinematics. Section 4 contains the conclusions. In the Appendix we collect some additional details of the calculation.

2 Details of the Calculation

2.1 General Framework

The process we want to consider in the following is the inclusive production of a pair of hadrons $H_1 H_2$ in collisions of longitudinally polarized leptons and nucleons with four-momenta as specified in Eq. (2). Both hadrons are required to be at high transverse momentum. As mentioned above, we consider only the direct part of the cross section, where the exchanged photon interacts as an elementary particle.

Since we want to perform the NLO calculation using largely analytical methods, we are limited to observing a hadron H_1 with transverse momentum $P_{T,1}$ and rapidity y_1 , together with hadron H_2 in the opposite hemisphere, its transverse momentum vector $\mathbf{P}_{T,2}$ constrained by z_H defined in Eq. (3), but otherwise unspecified kinematics. Assuming, as usual, factorization, we may then write the NLO expression for the corresponding spin-dependent cross section as a convolution of the non-perturbative parton distribution and fragmentation functions and the hard-scattering of the partons

$$\begin{aligned} \frac{d\Delta\sigma^{H_1 H_2}}{dP_{T,1} dy_1 dz_H} &\equiv \frac{1}{2} \left[\frac{d\sigma_{++}^{H_1 H_2}}{dP_{T,1} dy_1 dz_H} - \frac{d\sigma_{+-}^{H_1 H_2}}{dP_{T,1} dy_1 dz_H} \right] \quad (4) \\ &= \frac{2P_{T,1}}{S} \sum_{i,j,k} \int_{1-V+VW}^1 \frac{dz_1}{z_1} \int_{\frac{VW}{z_1}}^{1-\frac{1-V}{z_1}} \frac{dv}{v(1-v)} \int_{\frac{VW}{vz_1}}^1 \frac{dw}{w} \\ &\times \int_{z_{\min}}^{z_{\max}} \frac{dz}{z} \Delta f_{\gamma}^l(x_l, \mu_f) \Delta f_i^N(x_N, \mu_f) \frac{\alpha_s(\mu_r) \alpha_{em}}{s} \\ &\times \left[\frac{d\Delta\hat{\sigma}_{\gamma i \rightarrow jk}^{(0)}(v)}{dv} \delta(1-w) \delta(1-z) + \frac{\alpha_s(\mu_r)}{2\pi} \right. \\ &\times \left. \frac{d\Delta\hat{\sigma}_{\gamma i \rightarrow jkX}^{(1)}}{dv dw dz}(s, v, w, \mu_f, \mu'_f, \mu_r, z) \right] \\ &\times D_j^{H_1}(z_1, \mu'_f) D_k^{H_2}(z_2, \mu'_f). \quad (5) \end{aligned}$$

The subscripts “++” and “+-” in (4) denote the settings of the helicities of the incoming lepton and nucleon. We have introduced the standard hadronic invariants

$$S = (P_l + P_N)^2, \quad T = (P_l - P_1)^2, \quad U = (P_N - P_1)^2, \quad (6)$$

$$V = 1 + \frac{T}{S}, \quad W = -\frac{U}{S+T}, \quad (7)$$

with four-momenta specified in (2), and their partonic counterparts

$$s = (p_\gamma + p_i)^2, \quad t = (p_\gamma - p_j)^2, \quad u = (p_i - p_j)^2, \quad (8)$$

$$v = 1 + \frac{t}{s}, \quad w = -\frac{u}{s+t}. \quad (9)$$

Neglecting the masses of all particles one finds the following relations among the variables in Eqs. (6)-(9)

$$s = x_l x_N S, \quad t = \frac{x_l}{z_1} T, \quad u = \frac{x_N}{z_1} U, \quad (10)$$

$$x_l = \frac{VW}{vWz_1}, \quad x_N = \frac{1-V}{(1-v)z_1} \quad (11)$$

with $x_e [x_N]$ the fraction of the longitudinal momentum of the lepton [nucleon] taken by the quasi-real photon [parton i]. In addition, V and W in (7) are determined by the observed hadron H_1 and the lepton-nucleon c.m.s. energy squared S :

$$V = 1 - \frac{P_{T,1}}{\sqrt{S}} e^{-y_1}, \quad W = \frac{P_{T,1}^2}{SV(1-V)}. \quad (12)$$

In (5) we have also introduced the partonic counterpart of z_H , defined via

$$z = -\frac{\mathbf{p}_{T,j} \cdot \mathbf{p}_{T,k}}{p_{T,j}^2} = \frac{z_1}{z_2} z_H \quad (13)$$

with $p_{T,j}$ and $p_{T,k}$ the transverse momenta of the final-state partons i and j producing hadrons H_1 and H_2 , respectively. $z_{1,2}$ are the momentum share that the hadrons $H_{1,2}$ inherit from its parent partons j, k in the hadronization process. The latter is modeled by non-perturbative functions $D_{j,k}^{H_{1,2}}(z_{1,2}, \mu_f')$ describing the collinear fragmentation of the partons j and k into the observed hadrons H_1 and H_2 , respectively.

The $\Delta f_i^N(x_N, \mu_f)$ in (5) are the spin-dependent parton distribution functions, defined as usual by

$$\Delta f_i^N(x_N, \mu_f) = f_{i(+)}^N(x_N, \mu_f) - f_{i(-)}^N(x_N, \mu_f). \quad (14)$$

The subscript $+$ [$-$] in Eq. (14) indicates that the parton's spin is aligned [anti-aligned] with the spin of the parent nucleon N .

As we only focus on the direct photon case in our calculation, $\Delta f_\gamma^l(x_l, \mu_f)$ in (5) coincides with the spin-dependent Weizsäcker-Williams equivalent photon spectrum, which reads [17]

$$\begin{aligned} \Delta f_\gamma^l(x_l, \mu_f) &= \frac{\alpha_{em}}{2\pi} \left[\frac{1 - (1 - x_l)^2}{x_l} \ln \frac{Q_{max}^2(1 - x_l)}{m_l^2 x_l^2} \right. \\ &\quad \left. + 2m_l^2 x_l^2 \left(\frac{1}{Q_{max}^2} - \frac{1 - x_l}{m_l^2 x_l^2} \right) \right], \end{aligned} \quad (15)$$

with m_l the mass of the lepton. It describes the collinear emission of a photon with low virtuality Q , less than some upper limit Q_{max} determined by the experimental conditions. The non-logarithmic pieces in (15) result in a small but non-negligible contribution in case of muons.

The sum in (5) runs over all possible partonic channels $\gamma i \rightarrow jkX$, with $d\Delta\hat{\sigma}_{\gamma i \rightarrow jk}^{(0)}$ and $d\Delta\hat{\sigma}_{\gamma i \rightarrow jkX}^{(1)}$ the associated LO and NLO longitudinally polarized partonic hard-scattering cross sections, respectively. They are defined in complete analogy to Eq. (4) and have been stripped of trivial factors involving the electromagnetic coupling α_{em} and the strong coupling $\alpha_s(\mu_r)$ evaluated at renormalization scale μ_r . As indicated in (5), starting from the NLO level, the subprocess cross sections will explicitly depend on μ_r , as well as on the scales μ_f and μ_f' of the parton distribution and fragmentation functions owing to the factorization of initial and final-state collinear singularities to be discussed below. The calculation of the NLO $d\Delta\hat{\sigma}_{\gamma i \rightarrow jkX}^{(1)}/dvdwdz$ is the main purpose of the remainder of this paper.

A computation with largely analytical methods becomes feasible [10, 11, 12, 13] thanks to the introduction of the variable z (or z_H) describing H_2 . The price to pay is a limited control of the kinematics of hadron H_2 , most notably its rapidity y_2 . The main virtue of z is that when integrating over phase-space certain singular configurations of two partons can be easily avoided. For instance, momenta p_j parallel to p_k corresponds to negative values of z . In this case, the factorized expression (4) for the cross section is incomplete and contains uncanceled poles which would require the introduction of additional non-perturbative functions describing the simultaneous fragmentation of a single parton into two hadrons. Situations where hadron H_2 is parallel to the direction of the incoming photon are characterized by $z = 0$.

For the phase-space integrations of the matrix elements we therefore restrict ourselves to

$$z > z_{min} > 0, \quad (16)$$

equivalent to the condition that the two hadrons are produced by partons in opposite hemispheres. The final expressions for the subprocess cross sections will contain mathematical distributions in z , i.e., $\delta(1 - z)$, $1/(1 - z)_+$, etc., in addition to similar functions in the variable w , which are already present in the NLO computation of single-inclusive hadron spectra [18, 19]. The analytical results will therefore be rather involved and lengthy. Some technical details may be found in the Appendix.

Finally, we note that corresponding expressions for spin-averaged cross sections are straightforwardly obtained by replacing all polarized quantities in this subsection by their unpolarized counterparts. To the best of our knowledge, NLO corrections have not been computed with analytical methods in the unpolarized case either. We will therefore provide results also for $d\hat{\sigma}_{\gamma i \rightarrow jkX}^{(1)}/dvdwdz$.

2.2 LO Contributions

As we consider only the direct part of the photoproduction of two hadrons, there are only two partonic channels contributing to (5) in the lowest order approximation: photon-gluon fusion,

$$\gamma g \rightarrow q\bar{q}, \quad (17)$$

and the QCD Compton process,

$$\gamma q \rightarrow qg. \quad (18)$$

Since at LO $s + t + u = 0$ and $\mathbf{p}_{T,j} = -\mathbf{p}_{T,k}$, the partonic cross sections are δ -functions in w and z , i.e.,

$$\frac{d\Delta\hat{\sigma}_{\gamma i \rightarrow jk}^{(0)}}{dv dw dz} = \frac{d\Delta\hat{\sigma}_{\gamma i \rightarrow jk}^{(0)}}{dv} \delta(1-w)\delta(1-z) \quad (19)$$

as indicated in (5). The PGF process is symmetric under exchange of q and \bar{q} , and the result for $\gamma q \rightarrow qg$ can be obtained by replacing v by $1-v$. Explicit expressions for $d\Delta\hat{\sigma}_{\gamma i \rightarrow jk}^{(0)}$ can be found, e.g., in [18]. Phenomenological studies based on LO results have been performed, for instance, in [20] and, most recently, in [16]. The unpolarized counterparts $d\hat{\sigma}_{\gamma i \rightarrow jk}^{(0)}$ are given, e.g., in [21].

2.3 Computation of NLO Corrections

At NLO, three different types of contributions have to be considered and evaluated:

1. the interference of the tree-level amplitudes for the processes (17) and (18) and the virtual, one-loop corrections to them;
2. the real gluon emission corrections to the tree-level processes, i.e., $\gamma q \rightarrow qgg$ and $\gamma g \rightarrow q\bar{q}g$;
3. genuine NLO processes, i.e., $\gamma q \rightarrow q'\bar{q}'q$, $\gamma q \rightarrow q\bar{q}q$.

To account for singularities one encounters when calculating the loop diagrams or when performing the phase-space integrations for the unobserved parton, we use dimensional regularization, where space-time is extended to $n = 4 - 2\varepsilon$ dimensions. To project onto definite helicity states for the incoming parton and photon, we adopt the standard HVBm prescription [22] to define γ_5 and the Levi-Civita tensor in n dimensions. The relevant n -dimensional partonic hard-scattering matrix elements *before* integration over phase-space are the same as for single-inclusive particle or jet production and hence well known.

The virtual corrections can be found, e.g., in [18] and [21] in the polarized and unpolarized case, respectively. Since they resemble the two-body final-state of the LO result in (19), their contribution to the $\mathcal{O}(\alpha_{em}\alpha_s^2)$ corrections is proportional to $\delta(1-w)\delta(1-z)$. The polarized and unpolarized NLO matrix elements in n dimensions with a three-parton final-state can be taken from Refs. [18,21] as well. Integrating them analytically over the phase-space of the unobserved parton is, however, much more involved than for single-inclusive hadron production and special care has to be taken.

2.4 Phase-Space Integration

We consider a generic “2 \rightarrow 3” photoproduction process

$$\gamma(p_\gamma)i(p_i) \rightarrow j(p_j)k(p_k)l(p_l) \quad (20)$$

contributing to $d(\Delta)\hat{\sigma}_{\gamma i \rightarrow jkX}^{(1)}$ in Eq. (5). Partons j and k shall produce the two observed hadrons in the fragmentation process. Parton l remains unobserved and hence has to be integrated over the entire phase-space. The phase-space of one of the observed partons, say k , is constrained by z but otherwise integrated. We shall perform all integrations analytically and express the result in terms of the variables v , w , and z .

Starting from the definition of the three-particle phase-space in n dimensions

$$dPS_3 = \int \frac{d^n p_j}{(2\pi)^{n-1}} \frac{d^n p_k}{(2\pi)^{n-1}} \frac{d^n p_l}{(2\pi)^{n-1}} \delta(p_j^2)\delta(p_k^2)\delta(p_l^2) (2\pi)^n \delta^{(n)}(p_\gamma + p_i - p_j - p_k - p_l) \quad (21)$$

one proceeds at first along the same steps as for a one-particle inclusive final-state [23], arriving at the well-known result

$$dPS_3 = \frac{s}{(4\pi)^4 \Gamma(1-2\varepsilon)} \left[\frac{4\pi}{s} \right]^{2\varepsilon} v^{1-2\varepsilon} (1-v)^{-\varepsilon} dv \times [w(1-w)]^{-\varepsilon} dw \int d\theta_1 d\theta_2 (\sin\theta_1)^{1-2\varepsilon} (\sin\theta_2)^{-2\varepsilon}. \quad (22)$$

To proceed, we parametrize the momenta in (20) in the c.m.s. frame of partons k and l ,

$$p_k = \frac{\sqrt{s_{kl}}}{2} (1, p_x, \sin\theta_1 \cos\theta_2, \cos\theta_1, \hat{p}_k) \\ p_l = \frac{\sqrt{s_{kl}}}{2} (1, -p_x, -\sin\theta_1 \cos\theta_2, -\cos\theta_1, -\hat{p}_k), \quad (23)$$

where $s_{kl} = (p_k + p_l)^2 = sv(1-w)$. \hat{p}_k denotes the $(n-4)$ -dimensional components of p_k and p_x is arbitrary. The other three momenta can be chosen to have non-vanishing spatial components only in the y - and z -directions, and explicit parametrizations can be found in the Appendix. The variable z in (13) is introduced as

$$z \equiv m \cdot p_k \quad (24)$$

by defining an auxiliary space-like vector [10,11]

$$m \equiv \frac{p_\gamma u + p_i t + p_j s}{tu} \quad (25)$$

and using the identity

$$1 = \int dz \delta(z - m \cdot p_k) \quad (26)$$

to perform the integration over θ_1 in (22). One finally arrives at

$$dPS_3 = \frac{s}{(4\pi)^4 \Gamma(1-2\varepsilon)} \left[\frac{4\pi}{s} \right]^{2\varepsilon} v^{1-2\varepsilon} (1-v)^{-\varepsilon} dv \times [w(1-w)]^{-\varepsilon} dw dz 2\sqrt{\frac{w(1-v)}{1-vw}} \times \left[\frac{1-w+4w(1-v)z(1-z)}{1-vw} \right]^{-\varepsilon} \int d\theta_2 \sin^{-2\varepsilon} \theta_2, \quad (27)$$

in agreement with the result given in [10,11]. Further integration over θ_2 depends on the various combinations of scalar products of parton's momenta appearing in the hard-scattering matrix elements. Structures with a complicated dependence on θ_2 have to be decomposed into a basic set of calculable integrals using momentum conservation and extensive partial fractioning. An extensive list of basic integrals can be found in [10,11,12,13] and need not be repeated here. We only note that after integration over θ_2 one ends up with “plus-distributions” both in w and in z . We refer to the Appendix and Refs. [10,11,12,13] for a more detailed discussion.

Equation (27) is sufficient for integrating the unpolarized matrix elements and most of the terms in the longitudinally polarized ones. In the latter case, an extra complication arises, however, from contributions proportional to the $(n-4)$ -dimensional components \hat{p}_k in (23), the so-called “hat-momenta”. We encounter terms in the polarized matrix elements which depending on \hat{p}_k^2 and require modifications to (27), since in its derivation we have assumed that the $(n-4)$ -dimensional part can be trivially integrated. Upon a careful re-examination of the steps leading to (27), we find that these contributions lead to a modified phase-space formula given by

$$\begin{aligned} d\widehat{PS}_3 = & (-\varepsilon) \frac{s^2}{(4\pi)^4 \Gamma(2-2\varepsilon)} \left[\frac{4\pi}{s} \right]^{2\varepsilon} v^{2-2\varepsilon} (1-v)^{-\varepsilon} dv \\ & \times (1-w)[w(1-w)]^{-\varepsilon} dw dz \sqrt{\frac{w(1-v)}{1-vw}} \\ & \times \left[\frac{1-w+4w(1-v)z(1-z)}{1-vw} \right]^{1-\varepsilon} \int d\theta_2 \sin^{2-2\varepsilon} \theta_2, \quad (28) \end{aligned}$$

in agreement with the result given in Ref. [13]¹. As is explicit in (28), all contributions stemming from \hat{p}_k^2 are of $\mathcal{O}(\varepsilon)$ as they should. Nevertheless, they can lead to finite contributions in the limit $\varepsilon \rightarrow 0$ whenever they pick up a $1/\varepsilon$ pole in the remaining phase-space integrations.

2.5 Factorization and Final Results

Adding the renormalized virtual corrections and the real contributions, all infrared singularities cancel out, including all $1/\varepsilon^2$ terms. The remaining $1/\varepsilon$ singularities are of collinear origin and arise when the momentum p_l of the unobserved parton l becomes parallel to any of the other parton momenta. Singular configurations related to the initial-state are absorbed at a factorization scale μ_f into the definition of the parton densities. Similarly, final-state mass singularities are factorized at a scale μ'_f into the bare fragmentation functions. This is the essence of the factorization theorem. A special role play the singularities from a collinear splitting $\gamma \rightarrow q\bar{q}$, which are absorbed into the photon structure functions. Due to the freedom in choosing the amount of finite pieces subtracted along with

the pole terms, only the sum of direct and resolved photoproduction cross sections is independent of theoretical conventions at NLO and beyond. We choose the common $\overline{\text{MS}}$ scheme throughout.

As already mentioned in Sec. 2.1, the main virtue of introducing the variable z and demanding $z > 0$ is to avoid certain singular contributions which are beyond the factorized framework outline here: (a), when the two produced hadrons are collinear, corresponding to negative values of z and (b), when hadron H_2 is produced parallel to the direction of the incoming photon, characterized by $z = 0$.

The factorization procedure is performed in the standard way [23] by adding an appropriate “counter cross section” $d\Delta\sigma^{fact}$ to each partonic subprocess. At NLO, with partons j and k being observed as hadrons H_1 and H_2 , there are in principle four possible collinear configurations, and $d\Delta\sigma^{fact}$ schematically reads

$$\begin{aligned} \frac{1}{sv} \frac{d\Delta\sigma^{fact}}{dv dw dz} = & -\frac{\alpha_s}{2\pi} \left[\frac{1}{sv} \Delta H_{m\gamma}[w, \mu_f] \frac{d\hat{\sigma}_{mi \rightarrow jk}^\varepsilon}{dv} [ws, v] \delta(1-z) \right. \\ & + \frac{1}{s(1-vw)} \Delta H_{mi} \left[\frac{1-v}{1-vw}, \mu_f \right] \\ & \times \frac{d\hat{\sigma}_{\gamma m \rightarrow jk}^\varepsilon}{dv} \left[\frac{1-v}{1-vw} s, vw \right] \delta(1-z) \\ & + \frac{1}{s(1-v+vw)} H_{jm} [1-v+vw, \mu'_f] \\ & \times \frac{d\hat{\sigma}_{\gamma i \rightarrow mk}^\varepsilon}{dv} \left[s, \frac{vw}{1-v+vw} \right] \delta(z_1-z) \\ & + \frac{1}{sv} H_{km} [z, \mu'_f] \frac{d\hat{\sigma}_{\gamma i \rightarrow jm}^\varepsilon}{dv} [s, v] \\ & \left. \times \theta(1-z) \delta(1-w) \right]. \quad (29) \end{aligned}$$

The $d\Delta\hat{\sigma}_{ab \rightarrow cd}^\varepsilon[\zeta s, \xi]/dv$ are the n -dimensional $2 \rightarrow 2$ cross sections for the process $ab \rightarrow cd$ to be found in the HVBM scheme in [24]. These cross sections are evaluated at some shifted kinematics denoted by $[\zeta s, \xi]$, since the collinear parton j takes away a certain fraction of the available momentum. Furthermore,

$$(\Delta)H_{ab}(\kappa, \mu) = -\frac{1}{\hat{\varepsilon}} (\Delta)P_{ab}(\kappa) \left(\frac{\mu^2}{Q^2} \right)^\varepsilon + (\Delta)h_{ab}(\kappa), \quad (30)$$

where $1/\hat{\varepsilon} = 1/\varepsilon - \gamma_E + \ln 4\pi$ in the $\overline{\text{MS}}$ scheme and $z_1 \equiv 1/(1-v+vw)$. In (30) the $(\Delta)P_{ab}(z)$ denote the usual unpolarized (polarized) one-loop splitting functions in four dimensions. Note that the unpolarized H_{ab} contributes to the factorization of final-state singularities since we do not consider the production of polarized hadrons. The functions $(\Delta)h_{ab}(\kappa)$ represent the freedom in choosing a factorization prescription, and they all vanish in the $\overline{\text{MS}}$ scheme, except for $\Delta h_{qq}(\kappa) = -16(1-\kappa)/3$ [25]. Needless to say that an equation similar to (30) holds in the unpolarized case.

¹ We note that some of the equations in the Appendix of Ref. [13] contain obvious misprints.

For all subprocesses, the final polarized (and unpolarized) partonic cross sections at NLO accuracy in (5) can be schematically cast into the following form

$$\begin{aligned} \frac{d\Delta\hat{\sigma}_{\gamma i \rightarrow jkX}^{(1)}}{dvdwdz} = & \Delta K_1(v, w)\delta(1-z) + \Delta K_2(v, w)\delta(z-z_1) \\ & + \Delta K_3(v, w)\frac{\theta(1-z)}{(1-z)_+} + \Delta K_4(v, w)\frac{\theta(z_1-z)}{(z_1-z)_+} \\ & + \Delta K_5(v, w)\frac{\theta(z-1)}{(z-1)_+} + \Delta K_6(v, w)\frac{\theta(z-z_1)}{(z-z_1)_+} \\ & + \Delta K_7(v, w)\left(\frac{\ln(1-z)}{1-z}\right)_+ \\ & + \Delta K_8(v, w, z). \end{aligned} \quad (31)$$

The coefficients ΔK_i , $i = 1, \dots, 8$, contain, in general, distributions in w , and they can be decomposed further as²

$$\begin{aligned} \Delta K_i(v, w) = & \Delta k_1(v)\delta(1-w) + \Delta k_2(v)\frac{1}{(1-w)_+} \\ & + \Delta k_3(v)\left(\frac{\ln(1-w)}{1-w}\right)_+ + \Delta k_4(v, w). \end{aligned} \quad (32)$$

For brevity we have suppressed any dependence on the renormalization and factorization scales in (31) and (32). Again, expressions similar to (31) and (32) hold for each unpolarized NLO partonic subprocess.

3 Phenomenological Results

We now turn to a brief numerical study of our results focussing on the relevance of the NLO corrections and the residual scale uncertainties for both the polarized and unpolarized cross section. We postpone a detailed phenomenological study to a future publication [14] until the resolved photon contribution becomes available as well. For our studies here, we choose the kinematical setup of the COMPASS experiment, which scatters a beam of polarized muons with an energy of $E_\mu = 160$ GeV off deuteron in a polarized ${}^6\text{LiD}$ solid-state target, corresponding to a lepton-nucleon c.m.s. energy of $\sqrt{S} \simeq 18$ GeV.

The results we show will be differential in the transverse momentum $P_{T,1}$ of hadron H_1 and integrated over the angular acceptance of the COMPASS experiment, i.e., covering scattering angles of less than 180 mrad. Using $y = -\ln \tan(\theta/2)$ this straightforwardly translates into a lower bound on the pseudo-rapidity y_1 for hadron H_1 . Kinematics dictates the upper bound, depending on the hadron's transverse momentum $P_{T,1}$. Recall that we can not control the rapidity of hadron H_2 in our analytical calculation, which in turn implies that it may end up outside the acceptance of COMPASS. The range of the transverse momentum vector $\mathbf{P}_{T,2}$ of H_2 is restricted by demanding

$z_H > 0.4$, with z_H defined in Eq. (3). The momentum distribution of the quasi-real photons radiated off the muons is described by the Weizsäcker-Williams spectrum given in (15), with $m_l = m_\mu$ and $Q_{\text{max}}^2 = 0.5 \text{ GeV}^2$. The photon's momentum fraction x_l is restricted to be in the range $0.1 \leq x_l \leq 0.9$.

In the computation of the LO and NLO unpolarized cross section we use the LO and NLO CTEQ6 parton densities [26] and strong coupling α_s , respectively. In the polarized case, we use a special set of the GRSV helicity-dependent parton densities [27], characterized by a small negative total gluon polarization of $\Delta g = -0.15$ at the low input scale of GRSV. A small gluon polarization, either positive or negative, is indicated by all presently available data sensitive to $\Delta g(x, \mu_f)$ [1, 2, 3, 4], at least in the range of momentum fractions predominantly probed by these experiments, which roughly amounts to $0.05 \lesssim x \lesssim 0.2$. We note that for a set with a small positive gluon polarization, like the “standard scenario” of GRSV [27], which is also in agreement with current data, one encounters strong cancellations between the contributions from PGF and the Compton process, leading to sign changes in the polarized cross section. This makes it rather awkward to display the results for the NLO corrections and the scale dependence we are interested in here. Hence, for our purposes we resort to the choice of $\Delta g = -0.15$. In the forthcoming publication [14], we will discuss in detail the sensitivity of two-hadron photoproduction to $\Delta g(x, \mu_f)$.

To model the hadronization of partons j and k into the observed hadrons H_1 and H_2 , we use the novel set of fragmentation functions of DSS [28]. This new set is based on a first global QCD analysis of inclusive hadron spectra in electron-positron annihilation, DIS multiplicities, and hadron-hadron scattering and known to describe hadronization fairly well also in the energy range relevant for COMPASS [28]. Since COMPASS does not identify different hadron species [4] and measures only the sum of charged hadrons, we use the appropriate LO and NLO sets of DSS [28] for all our calculations.

Figure 1 shows our results for the $P_{T,1}$ -differential cross section for the polarized and unpolarized photoproduction of a pair of charged hadrons at LO and NLO accuracy at COMPASS. We have set all renormalization and factorization scales in (5) equal to twice the transverse momentum of hadron H_1 . The sum of the transverse momenta of both hadrons might be a better motivated choice, but we have no control over $P_{T,2}$ within our analytical calculation. The so-called “ K -factor”, defined as the ratio of NLO to LO unpolarized (polarized) cross sections

$$K \equiv \frac{d(\Delta)\sigma^{\text{NLO}}}{d(\Delta)\sigma^{\text{LO}}}, \quad (33)$$

is depicted in the lower panel of Fig. 1. The computed QCD corrections are such that the NLO results are below the LO estimates in the entire range of $P_{T,1}$ shown in Fig. 1. They appear to be more sizable in case of the polarized cross section. The observed difference of the unpolarized and polarized K -factors clearly indicates that NLO corrections are relevant also for studies of double-

² The coefficients $(\Delta)K_i$ are too lengthy to be given here, but are available upon request from the authors.

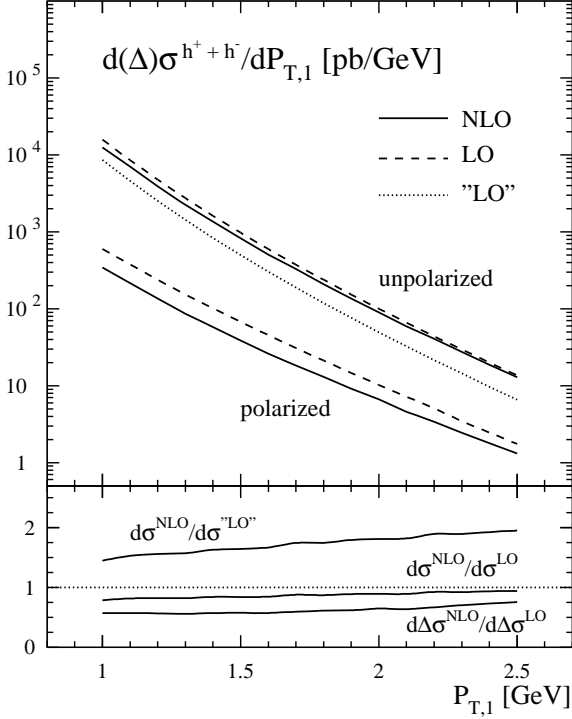


Fig. 1. Upper panel: unpolarized and polarized photoproduction cross section for a pair of charged hadrons, $\mu d \rightarrow (h^+ + h^-)(h^+ + h^-)X$, at LO (dashed line) and NLO (solid line) accuracy using COMPASS kinematics. The dotted curve labeled “LO” refers to a LO calculation using NLO parton densities and fragmentation functions (see text). The lower panel shows the corresponding ratios of NLO to LO cross sections (K -factor).

spin asymmetries, $A_{LL} \equiv d\Delta\sigma/d\sigma$, as they do not cancel in the ratio. The contrary is often *assumed* in analyses of spin asymmetries.

We wish to make two further remarks about the results shown in Fig. 1. Firstly, finding K -factors smaller than one is *not* a result of the NLO corrections to the hard-scattering partonic cross sections. It mostly stems from the difference between the LO and NLO parton distribution and fragmentation functions, in particular the latter. The LO and NLO sets of DSS show pronounced differences, mainly because the LO fragmentation functions try to make up for the often large NLO corrections in some of the fitted cross sections, see [28] for details, which are missing in a consistent LO analysis. The effect of the fragmentation functions is illustrated in Fig. 1 in the unpolarized case by the curves labeled “LO”. They refer to a calculation using LO matrix elements, but NLO parton densities and fragmentation functions. This clearly demonstrates the inadequacy of LO results. At best, they can serve as a rough estimate, but they are insufficient for any quantitative analysis. Very similar observations can be made in the polarized case. Here, a “LO”-type calculation leads to K -factors ranging from 1.1 to 1.8 (not shown in Fig. 1 for clarity). Secondly, we note that the details and size of the NLO corrections in the polarized case de-

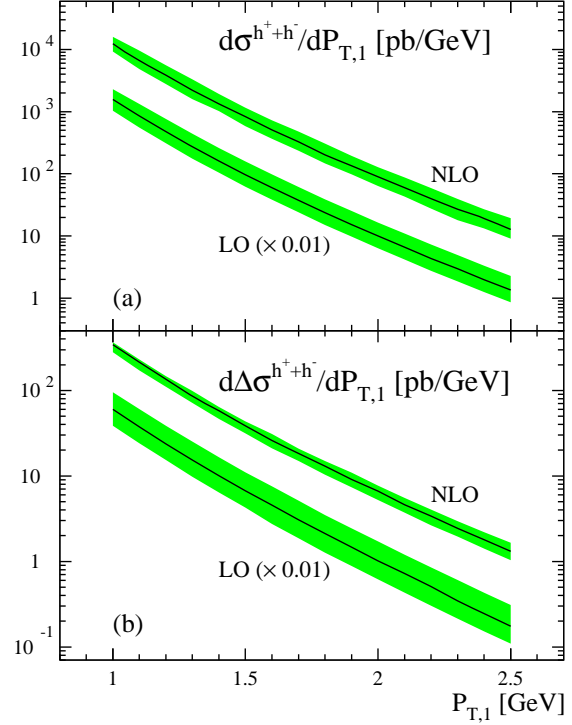


Fig. 2. Scale dependence of the LO and NLO unpolarized (a) and polarized (b) cross sections for $\mu d \rightarrow (h^+ + h^-)(h^+ + h^-)X$ shown in Fig. 1. All scales are varied simultaneously in the range $\sqrt{2}P_{T,1} \leq \mu_r = \mu_f = \mu'_f \leq 2\sqrt{2}P_{T,1}$. Solid lines correspond to the choice where all scales are set to $2P_{T,1}$. All LO computations have been rescaled by a factor 0.01 to better distinguish them from the NLO results.

pend significantly on the still largely unknown gluon polarization. As already mentioned, there can be strong cancellations between different subprocesses, leading to sign changes in the polarized cross section. In their vicinity large NLO corrections are in general inevitable.

As an estimate for the sensitivity of the computed cross sections to the actual choice of scales μ_f , μ'_f , and μ_r in (5), we vary them simultaneously in the range $\sqrt{2}P_{T,1} \leq \mu_r = \mu_f = \mu'_f \leq 2\sqrt{2}P_{T,1}$. We note that in principle all scales can be varied independently. The shaded bands in Figs. 2 (a) and (b) indicate the resulting residual scale uncertainty of the unpolarized and polarized photoproduction cross sections, respectively. We find that the NLO results show somewhat reduced theoretical ambiguities, in particular, for the polarized cross section. However, similar remarks as above apply also here. Scale ambiguities in the polarized case depend on the details of the helicity-dependent parton densities and on possible cancellations among different subprocesses. One also has to keep in mind that the results so far only include the direct photon contribution to the photoproduction cross section. It remains to be seen what the effects of the resolved photon contribution are. We will address all these questions in a forthcoming publication.

4 Summary and Conclusions

To summarize, we have computed, with largely analytical methods, the NLO QCD corrections to the direct part of the spin-dependent cross section for hadron-pair photoproduction. This is the first step towards a full NLO description of this process, which plays an important phenomenological role in the determination of the gluon polarization in polarized lepton-nucleon collisions studied by HERMES and COMPASS at present and, hopefully, at higher c.m.s. energies at some facility like eRHIC in the future.

We find that the NLO corrections are essential for any study of double-spin asymmetries. They are sizable and do not cancel in the ratio. Theoretical ambiguities due to the choice of the arbitrary renormalization and factorization scales are somewhat reduced if NLO corrections are taken into account.

Acknowledgements

C.H. was supported by a grant of the “Bayerische Eliteförderung”. This work was supported in part by the “Deutsche Forschungsgemeinschaft (DFG)”.

Appendix

Parametrization of Momenta

To perform the phase-space integration over the angle θ_2 for all $2 \rightarrow 3$ subprocesses $\gamma i \rightarrow jkl$ analytically, we choose to work in the c.m.s. frame of the observed parton k and the unobserved parton l . Their momenta are parametrized in Eq. (23). All partons are assumed to be massless. The remaining three momenta are chosen in such a way that they have non-vanishing components only in two spatial directions:

$$\begin{aligned} p_\gamma &= \frac{sv}{2\sqrt{s_{kl}}}(1, 0, \sin\psi, \cos\psi, \dots), \\ p_i &= \frac{s(1-vw)}{2\sqrt{s_{kl}}}(1, 0, -\sin\psi, \cos\psi, \dots), \\ p_j &= \frac{s(1-v+vw)}{2\sqrt{s_{kl}}}(1, 0, \sin\psi', \cos\psi', \dots). \end{aligned} \quad (34)$$

The ellipsis in (34) denote zeros in $(n-4)$ -dimensional components, $s_{kl} = sv(1-w)$, and where

$$\begin{aligned} \cos\psi &= \sqrt{\frac{w(1-v)}{1-vw}}, \\ \sin\psi &= \sqrt{\frac{1-w}{1-vw}}, \\ \cos\psi' &= \frac{1+v-vw}{1-v+vw} \cos\psi, \\ \sin\psi' &= -\frac{1-v-vw}{1-v+vw} \sin\psi, \end{aligned} \quad (35)$$

with v and w defined in (9).

The five momenta can be used to define ten different scalar products or Mandelstam variables. Due to momentum conservation, $p_\gamma + p_i = p_j + p_k + p_l$, only five of the ten scalar products are independent. We make extensive use of all the relations among different Mandelstam variables to reduce the NLO matrix elements to a form amenable to analytic integration.

In the parametrization (23) and (34), the auxiliary vector m , introduced in (25), reads

$$m = \sqrt{\frac{s}{tu}} \left(\sqrt{\frac{w(1-v)}{1-w}}, 0, 0, \sqrt{\frac{1-vw}{1-w}}, \dots \right). \quad (36)$$

Plus-Distributions

In the analytic calculation for two-hadron production one encounters not only the usual plus-distributions in the variable w [23], but also a host of distributions in z , the partonic counterpart of z_H , as indicated in Eqs. (29) and (31). For completeness, we collect here only some of the definitions and identities, more details can be found in Refs. [10, 11, 12, 13].

With the common definition of plus-distributions via some arbitrary test function $f(z)$ [23], one has

$$\begin{aligned} \int_0^{z_1} dz \frac{f(z)}{(z_1 - z)_+} &\equiv \int_0^{z_1} dz \frac{f(z_1) - f(z)}{z_1 - z}, \\ \int_{z_1}^{z_{\max}} dz \frac{f(z)}{(z - z_1)_+} &\equiv \int_{z_1}^{z_{\max}} dz \frac{f(z) - f(z_1)}{z - z_1}, \end{aligned} \quad (37)$$

where $z_1 = 1/(1-v+vw)$ and z_{\max} the upper kinematical limit for the z -integration in (5),

$$z_{\max} = \frac{1}{2} \left[1 + \left(\frac{w(1-v)}{1-vw} \right)^{-1/2} \right]. \quad (38)$$

Analogously, the definition of other plus-distributions is obtained by replacing z_1 by 1 in (37).

Note that in the case $w = 1$, the upper integration limit (38) of z becomes $z_{\max} = 1$, and the distributions at $z = z_1$ coincide with the distributions at $z = 1$. Also, in the region $z > 1$, the variable w is limited to $w < 1$, and distributions $1/(1-w)_+$ reduce to ordinary functions. Finally, the lower limit z_{\min} for the integration over z in (5) is a function of z_H and the other integration variables, giving rise to additional logarithmic contributions, e.g.,

$$\frac{1}{(z_1 - z)_+} = \frac{1}{(z_1 - z)_{z_{\min}}} + \delta(z_1 - z) \ln(z_1 - z_{\min}), \quad (39)$$

where the new distribution is defined by

$$\int_{z_{\min}}^{z_1} \frac{f(z)}{(z_1 - z)_{z_{\min}}} dz \equiv \int_{z_{\min}}^{z_1} \frac{f(z) - f(z_1)}{z_1 - z} dz. \quad (40)$$

References

1. PHENIX Collaboration, A. Adare *et al.*, Phys. Rev. **D76**, 051106 (2007); STAR Collaboration, B.I. Abelev *et al.*, [arXiv:0710.2048 \[hep-ex\]](#).
2. HERMES Collaboration, A. Airapetian *et al.*, Phys. Rev. Lett. **84**, 2584 (2000); Spin Muon Collaboration (SMC), B. Adeva *et al.*, Phys. Rev. **D70**, 012002 (2004).
3. P. Liebing (for the HERMES Collaboration), AIP Conf. Proc. **915**, 331 (2007).
4. COMPASS Collaboration, E.S. Ageev *et al.*, Phys. Lett. **B633**, 25 (2006).
5. COMPASS Collaboration, M. Alekseev *et al.*, [arXiv:0802.3023 \[hep-ex\]](#).
6. See, for example: G. Bunce, N. Saito, J. Soffer, and W. Vogelsang, Annu. Rev. Nucl. Part. Sci. **50**, 525 (2000); C. Aidala *et al.*, *Research Plan for Spin Physics at RHIC*, 2005, BNL report BNL-73798-2005.
7. D. de Florian, R. Sassot, M. Stratmann, and W. Vogelsang, to appear.
8. See <http://www.bnl.gov/eic> for information concerning the eRHIC/EIC project, including the “White Paper” prepared for the NSAC Long Range Plan 2007; A. Deshpande, R. Milner, R. Venugopalan, and W. Vogelsang, Ann. Rev. Nucl. Part. Sci. **55**, 165 (2005).
9. See, for example: M. Klasen, Rev. Mod. Phys. **74**, 1221 (2002).
10. P. Aurenche, R. Baier, A. Douiri, M. Fontannaz, and D. Schiff, Z. Phys. **C24**, 309 (1984).
11. P. Aurenche, R. Baier, A. Douiri, M. Fontannaz, and D. Schiff, Z. Phys. **C29**, 459 (1985).
12. E.L. Berger and L.E. Gordon, Phys. Rev. **D54**, 2279 (1996).
13. C. Coriano and L.E. Gordon, Nucl. Phys. **B469**, 202 (1996).
14. C. Hendlmeier, A. Schäfer, and M. Stratmann, work in progress.
15. J.F. Owens, Phys. Rev. **D65**, 034011 (2002); T. Binoth, J.Ph. Guillet, E. Pilon, and M. Werlen, Eur. Phys. J. **C24**, 245 (2002).
16. C. Hendlmeier, A. Schäfer, and M. Stratmann, Eur. Phys. J. **C48**, 135 (2006).
17. D. de Florian and S. Frixione, Phys. Lett. **B457**, 236 (1999).
18. D. de Florian and W. Vogelsang, Phys. Rev. **D57**, 4376 (1998); B. Jäger, M. Stratmann, and W. Vogelsang, Phys. Rev. **D68**, 114018 (2003); Eur. Phys. J. **C44**, 533 (2005).
19. B. Jäger, A. Schäfer, M. Stratmann, and W. Vogelsang, Phys. Rev. **D67**, 054005 (2003).
20. M. Fontannaz, B. Pire, and D. Schiff, Z. Phys. **C8**, 349 (1981); A. Bravar, D. von Harrach, and A. Kotzinian, Phys. Lett. **B421**, 349 (1998); J.J. Peralta, A.P. Contogouris, B. Kamal, and F. Lebessis, Phys. Rev. **D49**, 3148 (1994); G. Grispos, A.P. Contogouris, and G. Veropoulos, Phys. Rev. **D62**, 014023 (2000).
21. P. Aurenche, R. Baier, A. Douiri, M. Fontannaz, and D. Schiff, Nucl. Phys. **B286**, 553 (1987); L.E. Gordon, Phys. Rev. **D50**, 6753 (1994).
22. G. 't Hooft and M. Veltman, Nucl. Phys. **B44**, 189 (1977); P. Breitenlohner and D. Maison, Comm. Math. Phys. **52**, 11 (1977).
23. R.K. Ellis, M.A. Furman, H.E. Haber, and I. Hinchliffe, Nucl. Phys. **B173**, 397 (1980).
24. L.E. Gordon and W. Vogelsang, Phys. Rev. **D48**, 3136 (1993).
25. R. Mertig and W.L. van Neerven, Z. Phys. **C70**, 637 (1996); W. Vogelsang, Phys. Rev. **D54**, 2023 (1996); Nucl. Phys. **B475**, 47 (1996).
26. CTEQ Collaboration, J. Pumplin *et al.*, JHEP **0207**, 012 (2002).
27. M. Glück, E. Reya, M. Stratmann, and W. Vogelsang, Phys. Rev. **D63**, 094005 (2001).
28. D. de Florian, R. Sassot, and M. Stratmann, Phys. Rev. **D75**, 114010 (2007); **D76**, 074033 (2007).